Laboratori Nazionali di Frascati

LNF-64/70 (1964)

F. Amman, R. Andreani, M. Bassetti, M. Bernardini, A. Cattoni, R. Cerchia, V. Chimenti, G. Corazza, E. Ferlenghi, L. Mango, A. Massarotti, C. Pellegrini, M. Placidi, M. Puglisi, G. Renzler, F. Tazzioli:
STATUS REPORT ON THE 1.5 GeV ELECTRON POSITRON STORAGE RING - ADONE.

Estratto da: Proc. of the Intern. Conf. on High Energy Accelerators, Dubna 1963 (Atomirdat, Moscow, 1964) pag. 249.

64/70

STATUS REPORT ON THE 1.5 GeV ELECTRON POSITRON STORAGE RING—ADONE

F. Amman, R. Andreani, M. Bassetti, M. Bernardini, A. Cattoni, R. Cerchia, V. Chimenti, G. Corazza, E. Ferlenghi, L. Mango, A. Massarotti, C. Pellegrini, M. Placidi, M. Puglisi, G. Renzler, F. Tazzioli

Laboratori Nazionali di Frascati del CNEN, Italia

(Presented by F. AMMAN)

STORAGE RING DATA

Design Goals

Particles stored	e^+, e^-
Maximum energy	1.5 GeV
Intensity, per beam	2×10^{11} part.
Storage time	1—1.5 h
Beam crossing regions free for experiments	3 or 4
Interaction rate, per beam crossing region, for an event of total cross section 10^{-33} cm^2	10 events/h

Magnet

Focusing, type	AG, separ. funct.
Focusing, order	$O/2Q_FQ_DBQ_DQ_FO/2$
Field index, n, in bending magnets	0.5
Field, gradient in quadrupoles, at the max energy	~420 Gs/cm
Field, at injection	2.4 kGs
Field, at max energy	10 kGs
Bending radius	5 m
Mean ring radius	16.2 m
Number of periods	12
Betatron wave numbers	3.0—3.4
Closed orbit amplitudes, max	1.89 cm
for $\Delta p/p = 1\%$ min	0.96 cm
Momentum compaction	6.2×10^{-2}
Damping time constants, at injection	800 ms
for betatron oscillations at max energy	11 ms
Weight: iron	322 t
copper	31 t
Useful aperture: width	22 cm
height	6 cm

Injector system

Type	S-band linac
Injection energy, e^-	375 MeV
e^+	360 MeV
Injector current within e^-	25 mA
1% energy bin e^+	0.1 mA
Injection repetition rate, pulse per second	~0.6
Inflector type	C-loaded delay line

Vacuum system

Design pressure	10^{-9} Torr
Pumps, type	getter
Pumps, number and size	24×400 l/s

RF system

Frequency	8.9 MHz
Harmonic number	3
Accelerating cavities	2 or 3
Max. voltage per turn	180 or 250 kV
Input power to RF cavities	100 or 150 kW

1. INTRODUCTION AND GENERAL CONSIDERATIONS

The possibility of building a 1.5 GeV electron-positron storage ring has been considered at the Frascati National Laboratories since 1961, according to a proposal made by Prof. Touschek, of the Rome University, in the spring 1960. After about ten months the Study Group presented a preliminary proposal [1], which was approved by the National Institute of Nuclear Physics. The conclusion of the proposal was that, on the basis of the foreseeable positron current from a linac and of the little knowledge of the beam-beam interaction effects, it was more convenient to start with the construction of a ring of intermediate energy, say 750 MeV, before building the second one at 1.5 GeV.

A deeper study of the positron acceleration and a computation of the beam-beam interaction effects, convinced us that it was more convenient to build the 1.5 GeV ring without passing through the intermediate stage. Together with these technical arguments, there was an economic one: the separated function structure, which presented many advantages for a storage ring and was therefore chosen, altered completely the relative costs of the two rings. As a matter of fact the difference in cost bet-

ween the 750 MeV and the 1.5 GeV rings became so small (of the order of 10—15% of the overall cost of one complete ring) that a number of considerations which supported the solution of the two rings, lost any value.

At the end of 1962 it was then decided to build only the 1.5 GeV ring; very little of the

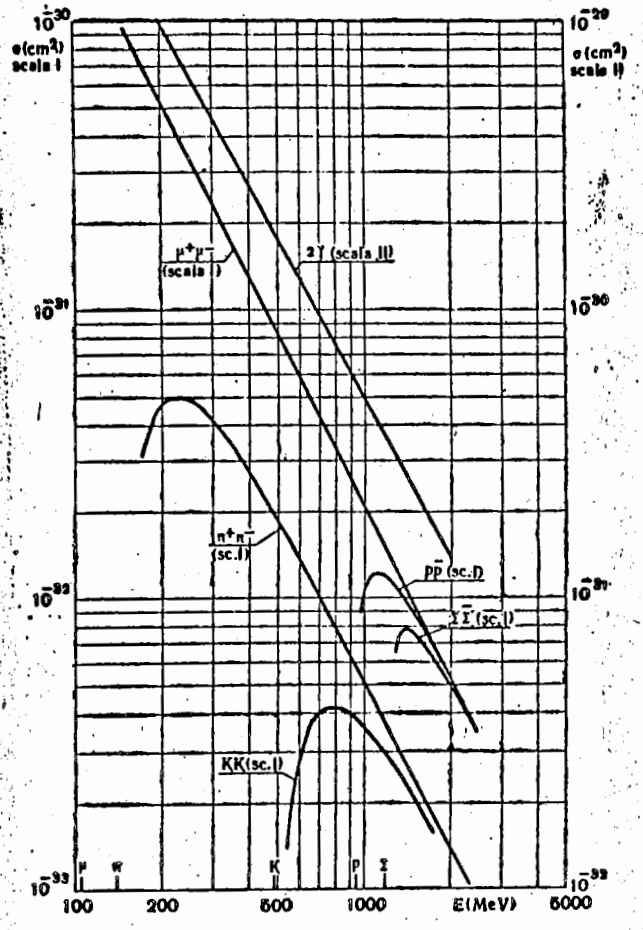

Fig. 1. Total annihilation cross sections in perturbation theory (from ref. [3]).

time spent on the design of the 750 MeV ring [2] has been wasted, as many of the parts are the same, or simply scaled. At present the project is entering in the final stage of actual construction: the injector has been recently ordered, tenders have been asked for the magnet and the construction of the buildings just started. The ring is scheduled to be completed by the end of 1965 or beginning of 1966: we think that it will take six months to get the storage ring operating smoothly, which means that the experiments should begin during the summer 1966.

We shall not say anything here about the use of such a machine; for this we refer mainly to the theoretical work done by Cabibbo and Gatto [3, 4]. Before going through a description of the different parts, let us consider briefly a few topics, characteristic of the storage rings, which led us to the design that will be presented in the following sections.

a) **Interaction rate and space charge effects.** The interaction rate per beam crossing region, $\dot{n}$ for an event whose cross section is σ (in cm²), is given by:

$$\dot{n} = \sigma f k \int_S \varrho_+ \varrho_- dS = L\sigma \text{ (events/sec)}, \qquad (1)$$

where f is the revolution frequency of the particles in the ring, k the RF harmonic number, ϱ_+ and ϱ_- the transverse densities of the two beams; the quantity L, measured in $cm^{-2} \cdot s^{-1}$ or $cm^{-2} \cdot h^{-1}$, includes all the ring parameters and is called luminosity.

The design goal for L is 10^{33} $cm^{-2} \cdot h^{-1}$, this value gives an interaction rate at the maximum energy of the order of units or tens per hour, depending on the type of reaction (Fig. 1). When the transverse density of the beams reaches a certain value, the spatial distribution of the particles in a beam is affected by the presence of the other beam; an increase of the transverse density tends first to increase the vertical dimensions of the beams, then to prevent the beams to cross, differentiating their mean orbits [5]. These space charge effects have been computed [6] for different values of the natural transverse density (i. e. the transverse density of one beam without space charge effects), assumed equal in the two beams, and of the vertical betatron phase shift μ between two adjacent crossing regions. As a result we obtained a set of universal curves, with parameter μ, which give the relative luminosity, L_{rel}, versus a quantity proportional to the natural transverse density, DE (Fig. 2); for «relative luminosity» we mean the ratio between the actual computed luminosity and the luminosity that would be obtained if the two beams crossed with their natural density distribution and completely overlapped.

It turned out that when μ is small (or close to a multiple of π), the transverse density that can be achieved, while keeping $L_{rel} \simeq 1$, is higher than when μ is large. This becomes

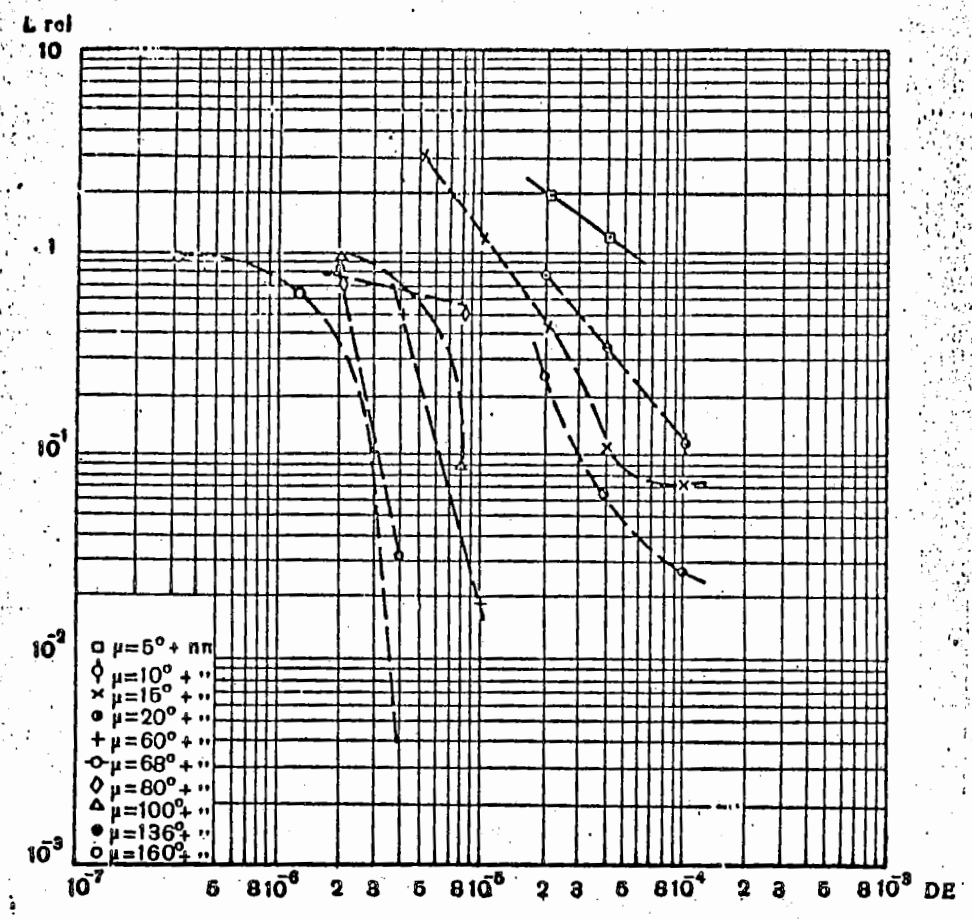

Fig. 2. Relative luminosity.

then a condition in the design of the focusing properties of the ring. With appropriate scale factors, that depend on the focusing properties and the energy, we can calculate the luminosity that can be achieved in a given storage ring for a given operating point (i. e. a certain value for μ and DE).

Fig. 3 shows a set of curves, versus energy, which refer to our ring: there is the space charge limited current I_{11m} and the corresponding luminosity L_{11m}, for the case when the beams have the natural dimensions; there is also the luminosity that can be obtained with the design value of the circulating current, 100 mA, and the factor $\mu = 100\ \text{mA}/I_{11m}$ by which in this case the beam dimensions must be increased to keep at the limit value the transverse density. This can be achieved either increasing the vertical dimensions, by coupling vertical and radial betatron oscillations, or making the beams to cross at an angle, by means of suitable electric fields distributed along the ring.

The natural dimensions of the beams are calculated according to ref. [7] and assuming a coupling of 1% between vertical and radial betatron oscillations, due to alignment errors; the vertical oscillation amplitudes are then 1% of the radial betatron oscillation amplitudes. The data in Fig. 3 refer to $\mu_v = 180° + 5°$, which corresponds to $\nu_v = 3.08$, and to $DE = 5 \times 10^{-5}$. A quantity which is important to know for the physicists who will use the machine for experiments, besides the expected interaction rate, is the energy probability distribution in an annihilation process. The rms value of the energy spread $\langle \overline{\Delta E^2} \rangle^{1/2}$ around $2E_s$, where E_s is the energy of the synchronous particle in one beam, is for our ring:

$$\frac{\langle \overline{\Delta E^2} \rangle^{1/2}}{2E_s} \simeq 3 \times 10^{-4} E_{\text{GeV}}. \qquad (2)$$

Eq. 2 shows one of the remarkable features of this type of experimentation: the exceptionally good energy resolution.

b) Type of focusing structure. As we saw before, the focusing structure should be such

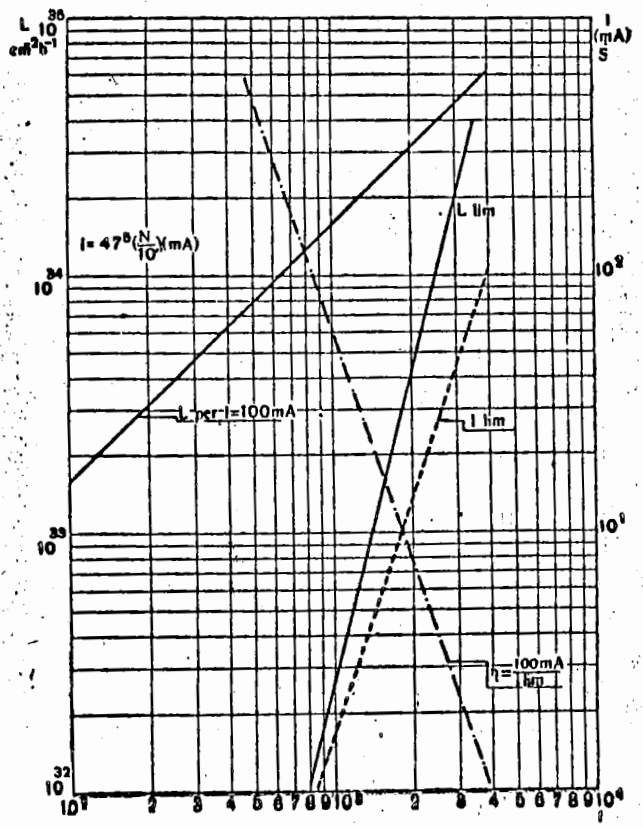

Fig. 3. Luminosity for the 1.5 GeV ring.

to give, for the vertical betatron oscillations, a wave number as close as possible to an integer or an integer plus one half. While this is the optimum operating point when the two beams cross each other with high transverse density, it might turn out to be an unstable operating point for one beam alone, or for two beams at low intensity, conditions which occur during injection. It is therefore very convenient to use a separated function structure, with low gradient bending magnets and quadrupoles, in which the betatron wave numbers can be changed, during operation, varying the currents in the quadrupoles.

Another advantage of the separated function structure, as compared to a conventional AG, is given by the fact that the three modes of oscillations (synchrotron, radial and vertical betatron) can be damped; when the field index n of the bending magnets is 0.5, the three damping coefficients do not depend on the focusing properties of the structure [7, 8]. As far as the focusing order is concerned, we find that in the straight sections, where both the injection and the beam crossings take place, the betatron amplitude functions, and β_{rad}, β_{vert} should have respectively a maximum and a minimum. The maximum for β_{rad} is required for the injection, as the inflector must be as far as possible from the equilibrium orbit, while a small value for β_{vert} increases the limit transverse density achievable in a crossing region and the vertical acceptance, allowing a smaller gap for the inflector.

These two conditions call for a symmetric structure, with the radial focusing elements close to the straight sections. The alignment requirements suggest to have the focusing and defocusing quadrupoles close together; the relative positions of the two elements of the doublet are critical, but they can be set with high accuracy, while the position of the doublet as compared to the ideal orbit need not to be very accurate. The number of periods is determined as follows. As we said the vertical betatron phase shift between two crossing regions must be:

$$\mu = n\pi + \varepsilon; \quad n \text{ integer}, \quad \varepsilon \ll 1. \qquad (3)$$

As we want that the crossings take place in the straight sections, n cannot be zero. Choosing $\pi/2$ as betatron phase shift per magnet period, and remembering that the number of beam crossings is equal to twice the RF harmonic number k, we have for N, the number of magnet periods:

$$N = 2k \frac{n\pi}{\pi/2} = 4kn. \qquad (4)$$

For a given number $2k$ of crossing regions, the smaller is N, the less expensive is the ring; the most convenient value for n is therefore 1. The choice of the number of crossing regions, where experiments and RF cavities are, must be done with a compromise between ring cost and convenience of having a large number of them; we decided to have six crossing regions ($k = 3$) of which two (or three) will be used for RF cavities and four (or three) for experiments. We note that for higher energy rings it would be convenient to use much higher RF harmonic numbers; if the possibility of zero angle beam crossing is given up, eq. 4 becomes:

$$N = 4 \frac{k}{m} n; \quad m \text{ integer} \qquad (5)$$

and the number of crossing regions is given by $2k/m$.

c) **Beam lifetime and injection efficiency.** Among the processes that contribute to the loss of the particles stored there are: bremsstrahlung and scattering on the residual gas, scattering of the particles in one beam [9]. It turns out that with the beam densities and the residual gas pressure which must be achieved in a storage ring, the last process gives the most severe limitation on the lifetime, specially at low energy.

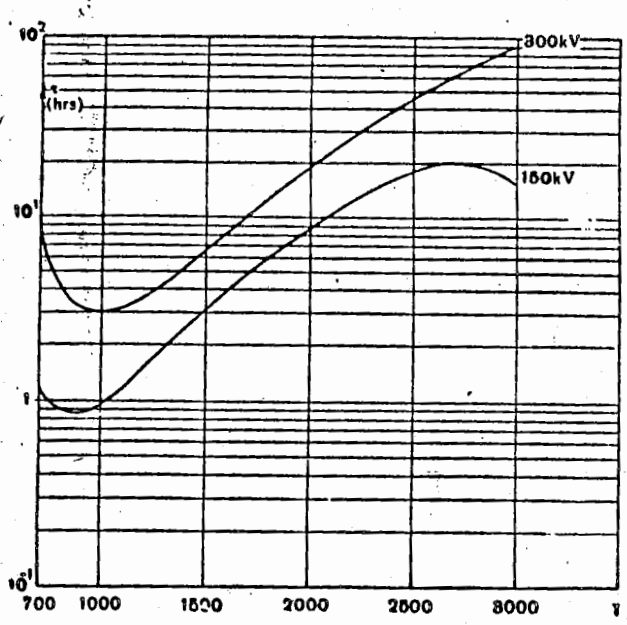

Fig. 4. Beam lifetime for scattering of the electrons in a bunch.

For a complete description and calculation of this process we refer to ref. [9] and [10]. The beam lifetime versus energy for our ring, for two values of the RF voltage, is given in Fig. 4; it is calculated taking into account the relativistic corrections and the correct distribution for the relative angles of the particles in one beam, but assuming that the distribution of the positions due to synchrotron oscillations is gaussian. The beam dimensions are the natural ones, as defined before (1% coupling between radial and vertical betatron oscillations) and the beam current has the design value of 100 mA, corresponding to about 2×10^{11} particles per beam. The error introduced because of the incorrect distribution of the positions due to synchrotron oscillations should not be very important (of the order of 10—20%); it can be inferred from the difference between this computation and the simplest one, made assuming a gaussian distribution for the relative angles.

From the diagrams in Fig. 4 we can draw a few considerations:

1. As the injection energy in our ring is 360 MeV and it will take 1 to 1.5 h to store 2×10^{11} electrons and positrons, the lifetime with 150 kV RF voltage is too short for the storage process; we must gain at least a factor 3—5. This can be easily achieved increasing the volume occupied by the beam, with a stronger coupling of the vertical and radial betatron oscillations, or increasing the length of the bunch, using an RF cavity at a higher harmonic of the principal ones.

2. The injection and capture efficiency has a maximum for a certain value of the RF voltage, much lower than 150 kV, if the average energy of the injected particles corresponds to the synchronous energy; the capture efficiency can be still high with 150 kV if the particles are injected with an energy different from the synchronous energy (a closed orbit closer to the inflector), but, in this case, as the betatron oscillation amplitudes are smaller, the number of turns that can be injected decreases, because the particles come back, where the inflector fringing field is high enough to cause their loss, after one or two turns.

3. The experimentation at low energy does not present particular problems because of the short lifetime: as a matter of fact the height of the beams can be increased by large factors, with stronger coupling of the oscillations, as we said talking of the beam-beam interaction, and the lifetime made proportionally longer; moreover the annihilation cross sections are larger at low energy, so that the ring could be used with lower intensities, therefore with longer lifetimes.

The points (1) and (2) above represent the most severe limitations on the operation of a storage ring with a low energy injection. We are now trying to find out the most convenient compromise between lifetime and storage time, computing the overall injection efficiency as a function of the RF voltage and position of the closed orbit of the injected particles; on the other side we are studying different systems to increase the beam volume. In the most pessimistic case we shall have an injection efficiency corresponding to one turn injection, 150 kV RF voltage and injection closed

orbit displaced as compared to the equilibrium orbit; in this case, with the assumption of a peak positron current from the linac within 1% energy bin equal to 100 μA, and with an injection pulse every two damping time constants, it will take less than one hour to store 2×10^{11} positrons.

2. INJECTOR AND INJECTION OPTICS

The injector is an *S*-band linear accelerator, specially designed for positron acceleration *. It will be built by a firm, Varian Ass. USA, and it should be installed in Frascati during the summer 1965. It is composed of two sections, with quite different characteristics: the high current section can accelerate an electron pulse current of 420 mA up to an energy of 65 MeV (unloaded energy 105 MeV); the high energy section can increase the energy of an electron beam current of 100 mA maximum by 280 MeV (unloaded energy 350 MeV).

For the positron acceleration, the electron beam, at the end of the high current section, is focused on a thick converter (~ 1 radiation length); a matching magnetic lens, with very short focal length, collects a fraction of the positrons produced, with a mean energy close to the critical energy (about 10 MeV); they are then accelerated in the high energy section. To increase its acceptance, the high energy section is surrounded by a solenoid which gives an axial field of 2.4 kGs. Assuming for the positron yield, the data of ref. [11], at 65 MeV primary energy we have, for the conversion efficiency:

$$\eta = 10^{-2} e^+/e^- \times \text{ster} \times \text{MeV}. \qquad (6)$$

The acceptance of the high energy section depends on the sizes of the iris useful region and of the positron source. As far as the iris useful region is concerned, at our best knowledge, no experimental data are available; with an iris diameter varying between 2.96 cm and 2.09 cm, the useful region for acceleration should probably be 1.5 cm to 2 cm in diameter.

The values of the accelerated positron current have been computed in different conditions of positron source size and of useful acceleration region size: the results in Table 1 assume that the electron beam current on the converter be equal to 420 mA, and consider the positrons coming out from the converter with energies between 7.5 and 12.5 MeV. The positron source is considered to have a gaussian density distribution, with rms radius equal to ϱ, and uniform distribution in angles and energy. The

Table 1

Positron current accelerated by the linac

R, mm	ϱ, mm	ΩΔE, ster×MeV	i_+, mA
10	0	0.45	1.9
10	1	0.33	1.4
10	1.6	0.22	0.92
7.5	0	0.25	1.05
7.5	1	0.145	0.61
7.5	1.6	0.087	0.37
5	0	0.113	0.47
5	1	0.047	0.20
5	1.6	0.026	0.11

R—radius of the useful acceleration region,
ϱ—rms radius of the positron source,
i_+—peak positron current accelerated.
Primary electron beam: 65 MeV—420 mA.
Axial magnetic field: 2.4 kGs.
Magnetic field in the matching lens: 17.7 kGs.

two values for ρ, 1 and 1.6 mm, correspond to the combination of a gaussian distribution for the incoming electron beam, with rms radius equal to 0.6 mm, with the lateral spread due to multiple scattering of 10 MeV electrons in a target $^1/_3$ and $^2/_3$ radiation length thick, respectively.

In our design, we assume that the peak positron current accelerated within 1% energy

Table 2

Linear accelerator data

	Electrons	Positrons
Energy, unloaded, MeV	440	360
Energy, for peak total current 100 mA, MeV	375	
Maximum total peak current, mA	100	~0.5
Peak current within 1% energy bin, mA	25	~0,1
Pulse duration: max, μs	3.2	
min μs	<0,01	
Pulse repetition rate: for 3.2 μs pulse duration, pulse per second	250	
for ⩽0,1 μs pulse duration, pulse per second	700	
Beam duty cycle, max	8×10^{-4}	
High current section: Energy, unloaded, MeV	105	
Energy, for peak total current 420 mA, MeV	65	
Maximum total peak current, mA	420	

* The linac construction is a program supported by CNR (National Research Council).

bin will be 100 μA. It is provided the possibility of modulating the beam current, at the linac cathode, with the ring RF frequency, 30% of the period on and 70% of the period off. This should allow a substantial increase of the capture efficiency in the ring and, as a consequence, should increase by some factor,

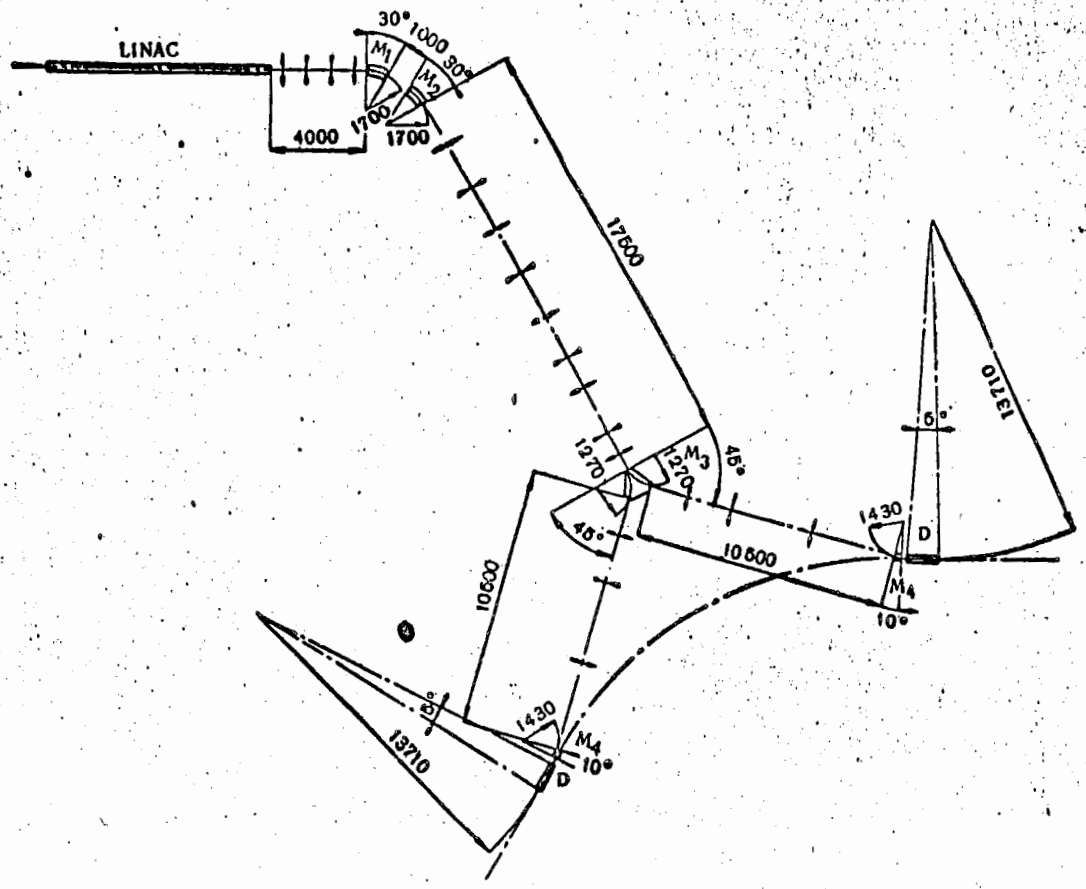

Fig. 5. Injection optics diagram.

of the order of 1.5 to 2, the charge stored per injection pulse. The linac will be used not only for injection in the ring, but also for experiments with the electron and positron beams. For this reason the repetition rate is much higher than that required for the injection; as a matter of fact its value is the maximum allowed by the klystrons. In Table 2 are summarized the principal data concerning the linac.

At the end of the high current section a deflecting magnet will allow to bring out the low energy, high current beam to an experimental hall; another bending magnet will be provided at the end of the linac to deflect the high energy beam to another experimental hall. A third bending magnet, at the end of the linac, deflects the accelerated beam towards the ring. The beam transport system from the linac to the ring, composed of magnets and quadrupoles, must satisfy three requirements:

1) the beams have to arrive tangent to the two injection straight sections;

2) the transport system must be achromatic, i. e. it must not introduce at the output correlations between energy of the particles and their angle or position;

3) the beam transverse emittance at the output of the transport system must have a certain definite shape, matched with the ring acceptance.

The design of the beam transport system has not yet been completed; up to now we found a few solutions (one is shown in Fig. 5) which

take into account only first order effects. The possible solutions will be compared taking into account higher order effects.

The criteria followed in the design are:

1) each deflection is made achromatic separately, by dividing in two parts the magnet and inserting in the middle a quadrupole; the two channels, for electrons and positrons, are therefore equal;

2) a solution satisfying the required conditions, except for the length between the two main deflections, is looked for;

3) the condition on the length is then satisfied inserting a quadrupole system which gives unit transfer matrix over its length.

3. PULSED INFLECTOR

The pulsed inflector is a four-wire delay line, loaded with capacitances, to lower its characteristic impedance. The requirements are: an inflection angle and a length such that a 400 MeV electron beam coming from the injector, at the input end of the injection straight section, be at a radial distance of 12 cm from the position of the beam at the output end of the inflector; there must be a region, whose cross section is $\sim$ 1 cm $\times$ 1 cm, where the deflecting field is constant within a 1% bin while the gap height is 2 cm; the current pulse must be $\sim$1.5—2 μs long, flat within 1% bin and with a decay time short compared to the revolution period of the electrons in the ring. The structure has been studied in the electrolytic tank first, and then with models on which electric measurements have been done.

The final model, in scale 1 : 1, is shown in Fig. 6; its length is 1.2 m and the magnetic field required is $\sim$950 Gs, which corresponds to 9.500 A; the characteristic impedance is 9.9 Ω, with VSWR $\leqslant$ 1.1 up to 30 MHz; the measured filling time is 45 ns. This values and the field plots, measured applying sinusoidal voltage at frequencies ranging from 0.1 to 10 MHz, agree very well with the calculated values and with the measurements in the electrolytic tank. In Fig. 7 a field plot is shown; it has been obtained with a differential coil system followed by an integrator. The region where B/B_0 is within 1% bin is a little smaller than initially required, namely 8 mm, and the fringing field has a more or less expo-

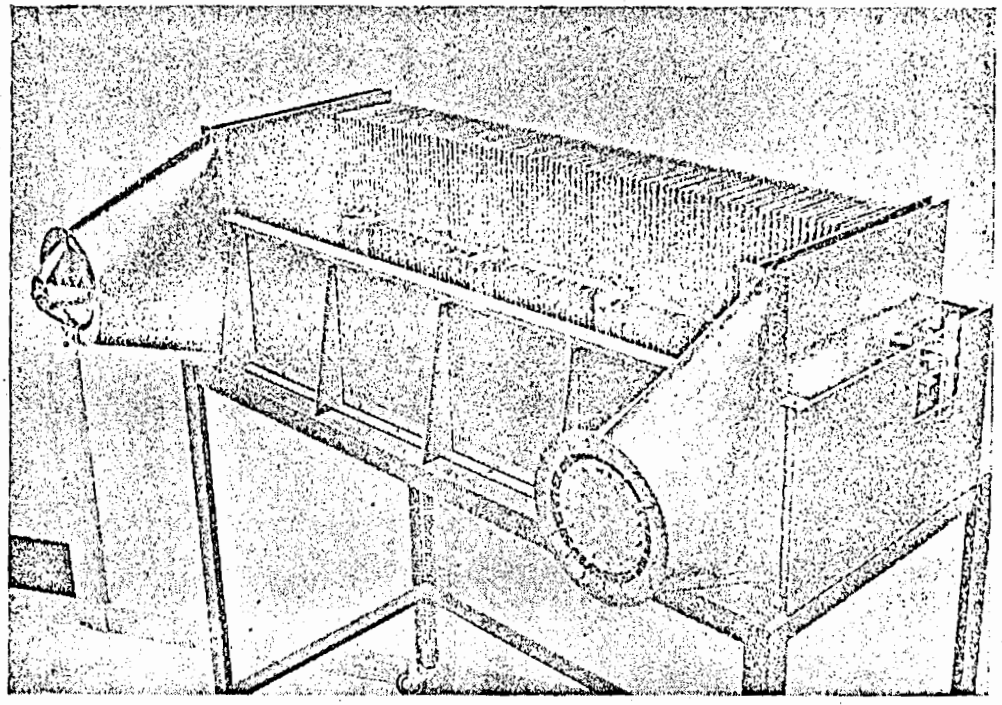

Fig. 6. Pulsed inflector model.

nential behaviour versus distance, falling to 1% of the central field at 4.6 cm from the inflector axis.

We are now preparing the construction of a prototype at full power. The pulse forming network, charged at about 200 kV, will be a cable; the switch, which must handle a peak flowing power of 1.000 MW, a spark gap. The matched load is designed for the peak power of 1.000 MW and an average power of 10 kW, corresponding to a pulse repetition rate of about 5 pulse per second.

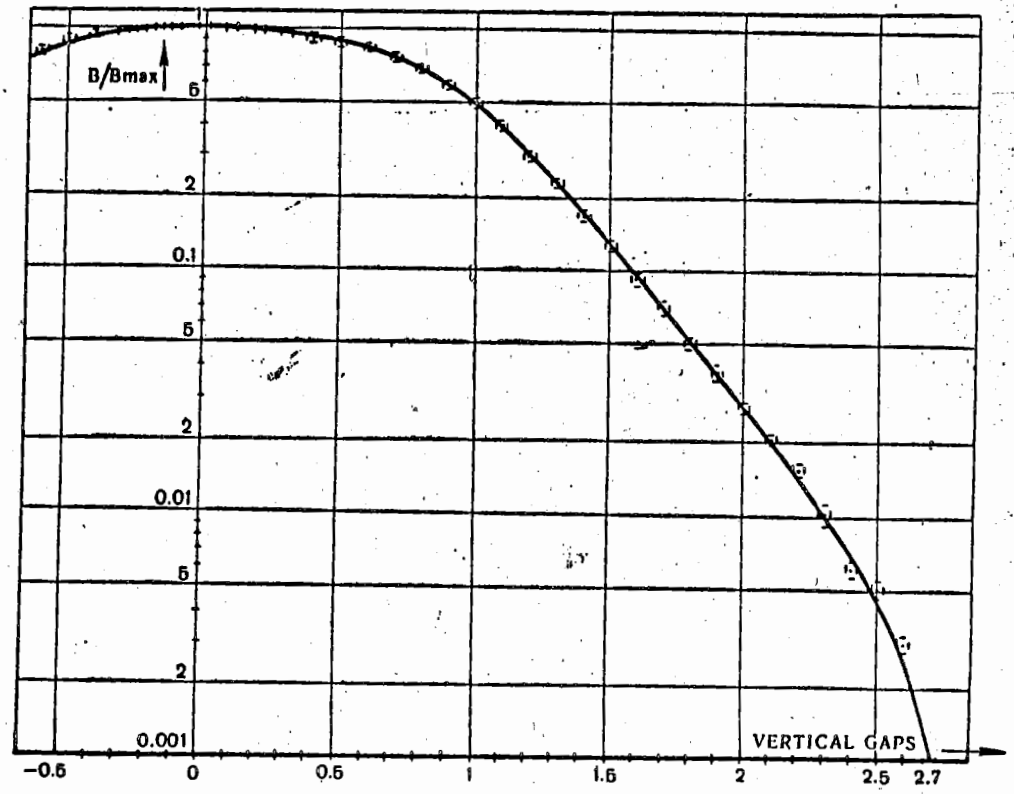

Fig. 7. Relative deflecting field in the pulsed inflector.

The technological problems associated with this type of pulsed inflector are certainly difficult to solve. They could have been easier if we required a smaller deflection angle, but we prefer to avoid the injection trough the fringing field of magnets or quadrupoles. A solution with a ferrite loading [12, 13] has been considered, but, while it has advantages from the electrical standpoint (lower voltage and current), it is much more difficult for the vacuum and the balance is in favour, at least for the time being, of the adopted solution.

4. MAGNET

The ring magnet structure has been chosen according to the above mentioned criteria; Fig. 8 and 9 show the ring layout and a view of a ring period. The straight sections are very long, 2.5 m, to allow enough room for experiments and for injection. Fig. 10 shows the amplitude functions, β_{rad} and β_{vert}, for radial and vertical betatron oscillations, and the closed orbit function, ψ, that is the local displacements, as compared to the synchronous orbit, of the closed orbit of a particle whose energy differs by 1% from the synchronous particle energy. Fig. 11 shows the betatron oscillation wave numbers versus the quadrupole strength K, which is defined as:

$$K = \frac{G}{B\varrho}\,(\mathrm{m}^{-2}), \tag{7}$$

$$K = 1\ \mathrm{m}^{-2} \quad \text{for} \quad G = 500\ \mathrm{Gs/cm},\quad E_s = 1.5\ \mathrm{GeV}, \tag{8}$$

where G is the quadrupole field gradient.

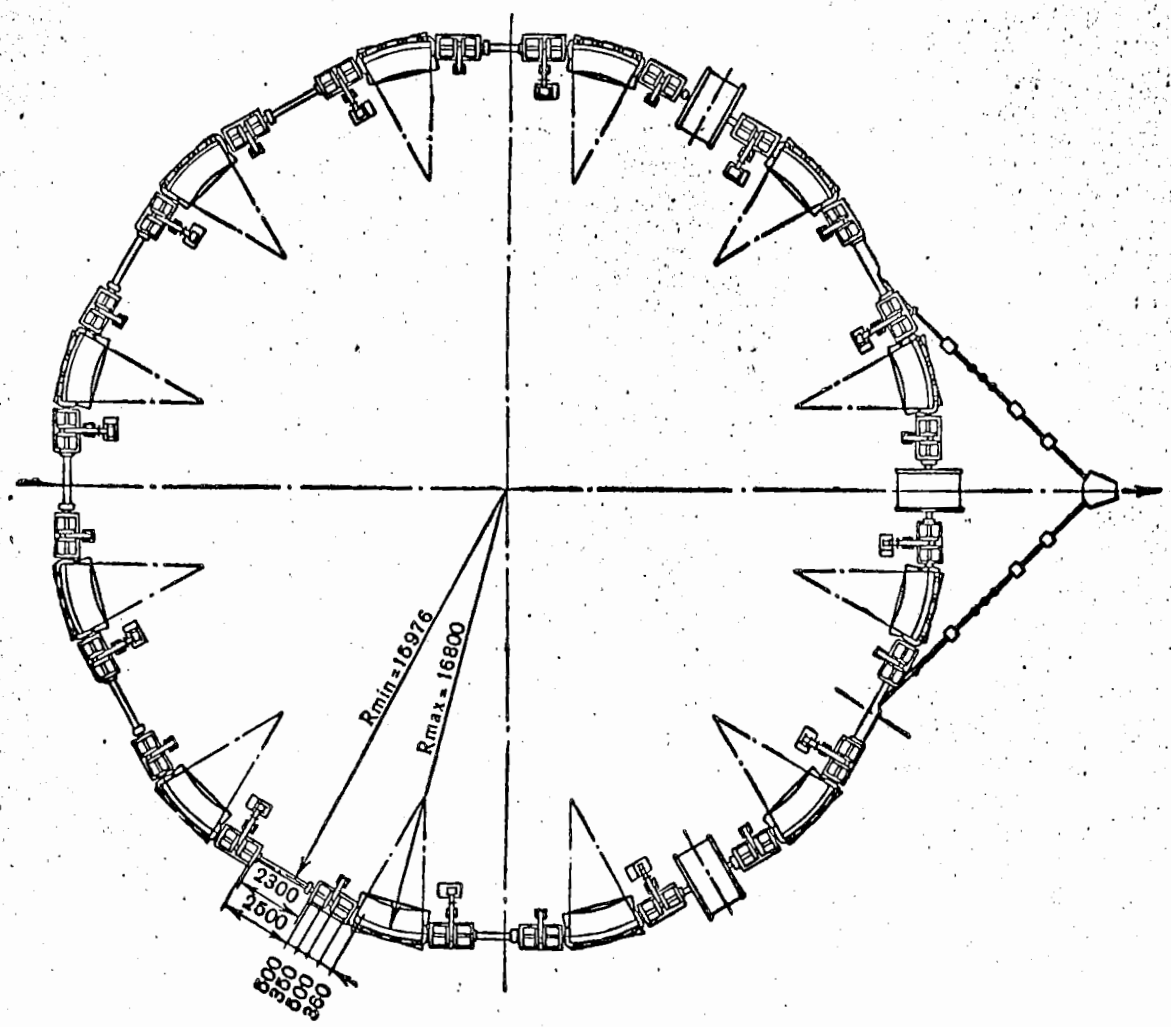

Fig. 8. Ring layout.

The ring radial useful aperture is chosen according to the injection requirements; as we already mentioned, we want that the stacked beam be not disturbed by the fringing field of the pulsed inflector; for a given height of the inflector (chosen taking into account the vertical emittance of the injected beam) and a given field in the inflector, we get a certain minimum distance between the inflector axis and the equilibrium orbit, which, in our case, turns out to be 6—7 cm.

A further allowance for the synchrotron oscillations, and for closed orbit shifts due to alignment errors, brings the required radial half aperture to our value of 11 cm. This large aperture is used only at the injection; when the beam is stored 6—7 cm would be enough (taking into account the RF stability region and the single scattering in the residual gas). The vertical half aperture is 1 cm in the straight section, where β_{vert} is minimum, and it is defined by the inflector height; this corresponds to about 2 cm in the middle of the bending magnet, where β_{vert} is maximum. Allowing room for heat insulation around the donut, and for a pair of electrodes in the donut, which give a vertical electric field, required to get the beam crossing at an angle and to sweep off the ions that might be trapped in the beam region, the magnet vertical half aperture becomes 5 cm. The magnet and the quadrupoles will be built in laminated iron, 1.5 mm thick; this has been decided to allow a field derivative with time of the order of 10 kGs/s.

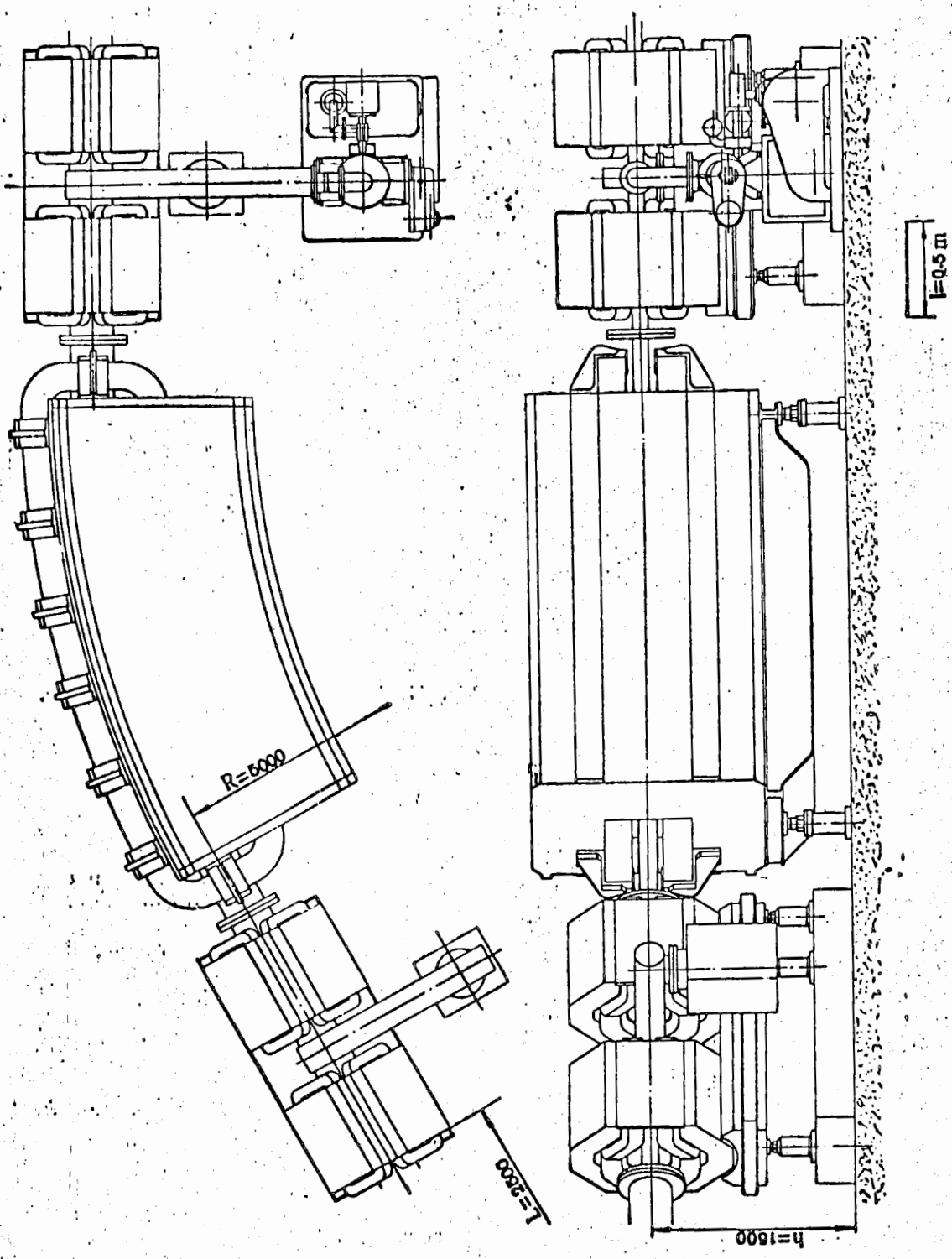

Fig. 9. View of a ring period.

The mechanical structure of the magnets si quite usual (Fig. 12); the quadrupoles (Fig. 13) have two unconventional features: they are not symmetric about the axis, as the required useful region is elliptic instead of circular, and they do not have return yokes on the sides, to avoid large masses of iron in the median

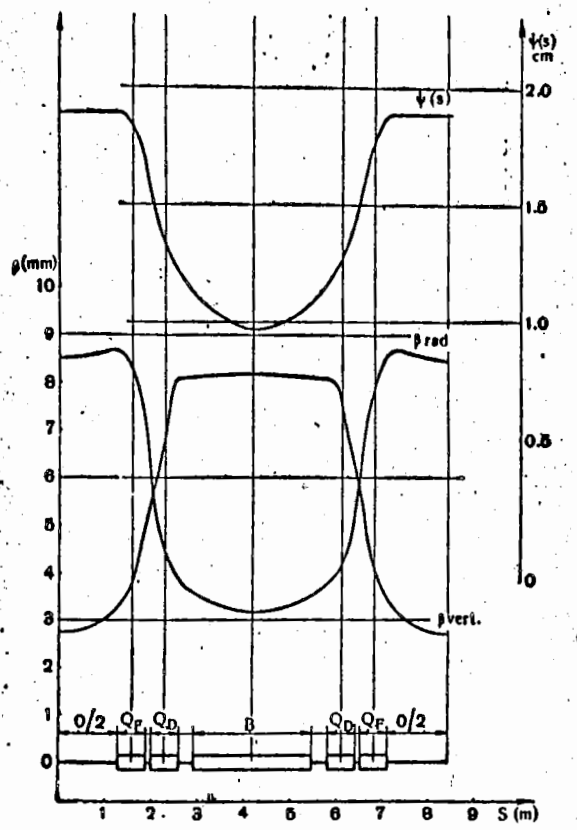

Fig. 10. Betatron amplitude and closed orbit functions.

plane close to the experimental regions, where showers due to lost electrons could be developed, contributing to the background of the experiments. Tenders have been asked for the construction of the bending magnets and quadrupoles; the construction should start before the end of the current year.

In Table 3 are summarized the alignment requirements for the magnetic elements [14]; it is given the root mean square value of the random displacements of the different elements which give an rms value of the closed orbit maximum displacement equal to 5 mm radially and 3 mm vertically. In the same table are also indicated the field gradient fluctuations, in the quadrupoles and bending magnets, which give an rms stopband width of 0.1, and the rms rotations around three axis of the different elements which give a coupling effect (that is a transfer of betatron amplitude) between radial and vertical oscillations equal to 10^{-2}, when the difference between radial and vertical betatron wave numbers is 0.05.

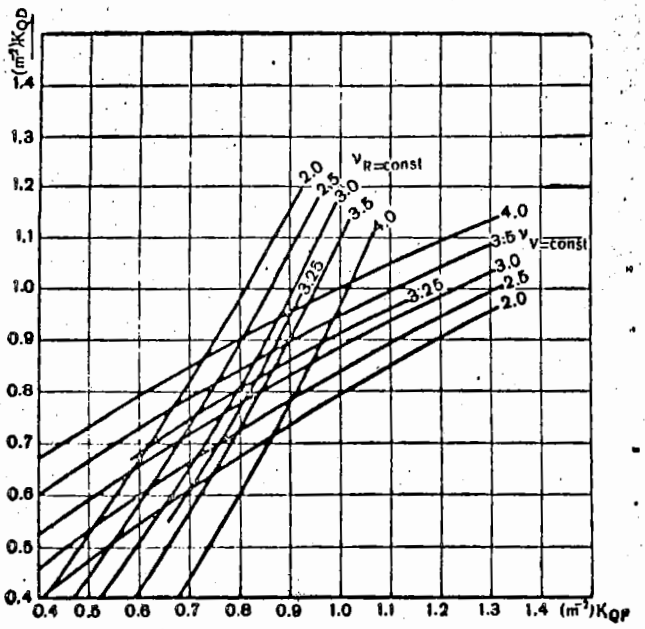

Fig. 11. Betatron oscillations ware numbers.

Tests of alignment procedure are under way; the first results [15] show that accuracies much higher than the ones indicated in Table 3 can be achieved in the alignment; the limit will then be set by the accuracy of the definition of the ideal orbit in each element, which will be obtained with magnetic measurements. Models of the bending magnets, in scale 1 : 2, and of the quadrupoles, in scale 1 : 1, have been built and tested (Fig. 14); the results are shown in Figs. 15 and 16. While the magnet profile can be considered the final one, the quadrupole needs still some change, as the gradient versus radial displacement is not constant enough.

The power supply will be composed of three independent rotating dc generators: one for the bending magnets, one for the focusing quadrupoles and one for the defocusing quadrupoles. The requirements for the current stability are stringent for the bending magnet generator, if we want to exploit the high energy resolution in colliding beam experiment. A current

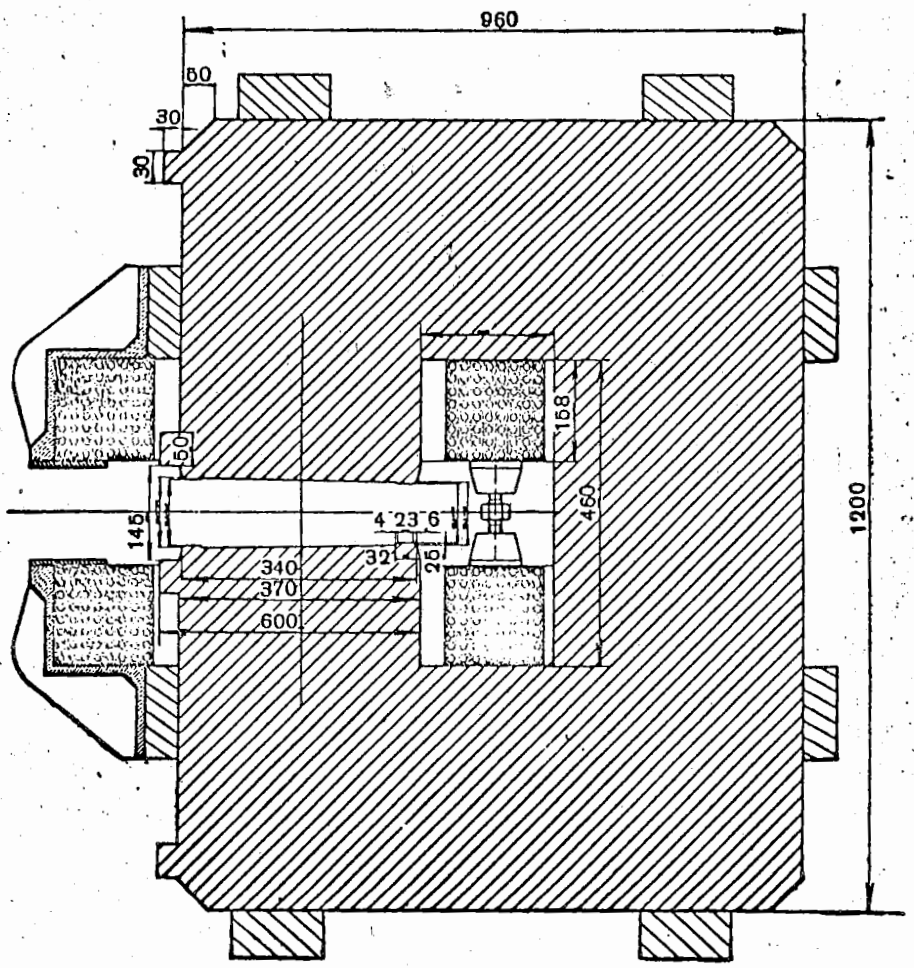

Fig. 12. Bending magnet cross section.

stability of the order of 5×10^{-4} is required, with the possibility of recording the current (or the magnetic field) with a sensitivity in the range of 10^{-5}.

5. THE VACUUM SYSTEM

The vacuum system must keep inside the donut a pressure less than 10^{-9} Torr. The system is composed of 24 getter pumps, with a pumping speed of 400 l/s each; 12 turbomolecular pumps, with a pumping speed of 140 l/s each, are provided for the outgassing of the donut. The molecular pumps will not be connected to the donut during regular operation, when the getter pumps will be on.

As it is shown in Fig. 9, the pumps will be connected to the donut between two quadrupoles; this solution has been chosen to let as much as possible of the room in the straight sections free for the experimental apparatus and the injection. The donut will be made of stainless steel type AISI 304, with copper gaskets; the dimensions relative to 1/12 of the ring are: length 8.42 m, volume 175 l, inner surface 4,43 m^2.

The donut parts will be subjected to the following treatments, after their construction:

a) cleaning with organic solvents (carbon tetrachloride),

b) electropolishing of the welds,

c) electrolytic degreasing, in hot alkaline baths,

d) passivation with hydrochloric acid,

e) cleaning in distilled water,

f) cleaning with alcohol or acetone.

The parts will then be assembled in the laboratory to form a sector (1/12 of the ring);

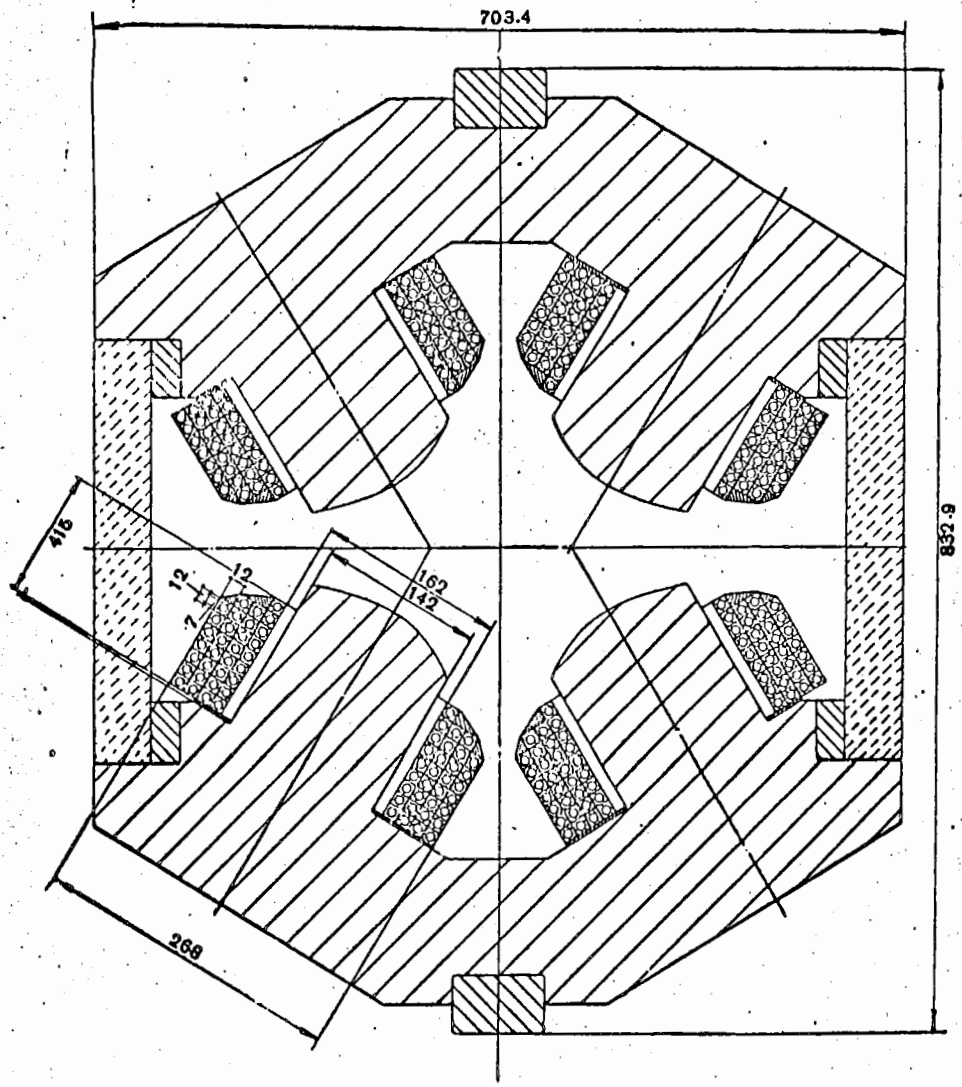

Fig. 13. Quadrupole cross section.

after a cold test for leaks, a sector will be heated up to 350—400° C for two days, pumped by a molecular pump and then let under vacuum with a getter pump. When the sectors shall be mounted together, they will be first filled with hydrogen and then let down to air and mounted.

A successive heating of the whole donut, within the magnet, up to 150° C for 3 to 6 h will allow to get a vacuum within the 10^{-10} Torr scale in a short time (one day or less). In the connection between the linac and the ring a differential pumping system will be mounted to account for the pressure difference of the two parts: 10^{-7} Torr in the linac and less than 10^{-9} Torr in the ring; it will be composed of three 75 l/s getter pumps. This system has already been tested in laboratory.

In Fig. 17 a prototype of half a sector, that is 1/24 of the whole ring, is shown during preliminary tests. It has been treated according to the above mentioned procedure; after the first outgassing at 350° C, it has been filled with hydrogen and then let down to air. A successive heating up to 150° C under vacuum for 3 h, allowed to reach a pressure equal to 10^{-9} Torr in 6 h. A reentry of argon, up to a pressure of 10^{-5} Torr, during 15', to regenerate

Fig. 14. Bending magnet and quadrupole models.

Table 3

Alignment and construction accuracy required

1) Closed orbit displacements

	Radial	Vertical
Rms value of the max closed orbit displacement assumed	5 mm	3 mm
Quadrupole rms relative displacement	0.09 mm	0.08 mm
Quadrupole doublets rms displacement	0.6 mm	0.5 mm
Bending magnets rms displacement	2.5 mm	1.3 mm
Bending magnets length rms dispersion	0.4 mm	—

2) Instability stopband

Stopband rms total width	$\langle \delta\nu^2 \rangle^{1/2} \leqslant$	0.1
Quadrupole gradient rms dispersion	$\left\langle \left(\frac{\Delta K}{K}\right)^2 \right\rangle^{1/2}$	0.65%
Bending magnet n rms dispersion	$\left\langle \left(\frac{\Delta n}{n}\right)^2 \right\rangle^{1/2}$	27%

3) Betatron oscillations coupling

Assumed value for the coupling, with $|\nu_r - \nu_v| = 0.05$ . . . . . 10^{-2}

Rotation around	Quadrupole	Bending Magnets
an azimuthal axis $\langle \varphi^2 \rangle^{1/2}$	2×10^{-3} rad	1.2×10^{-3} rad
a radial axis $\langle \varphi^2 \rangle^{1/2}$	6×10^{-3} »	1.7×10^{-3} »
a vertical axis $\langle \varphi^2 \rangle^{1/2}$	6×10^{-3} »	5×10^{-2} »

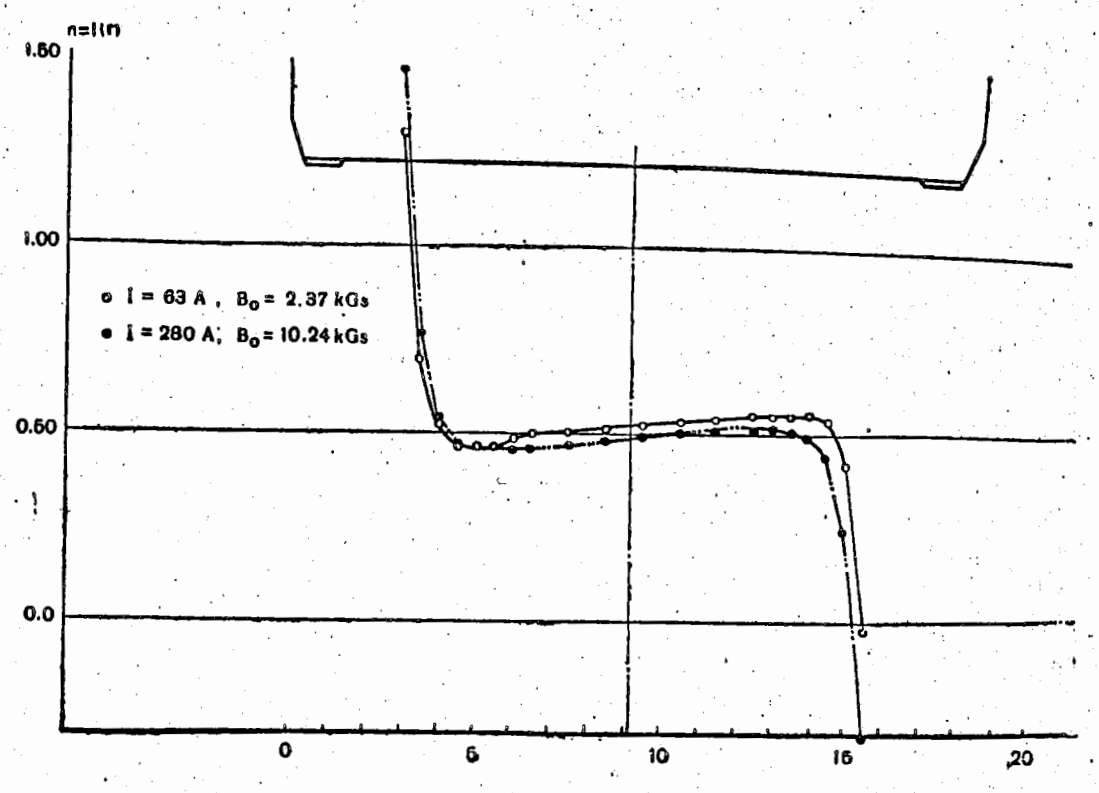

Fig. 15. Field index measured on the magnet model.

the getter pumps, made the pressure to go down in one day, to an average value of 2.5×10^{-10} Torr ($\sim 1.5 \times 10^{-10}$ at the pump and $\sim 3 \times \times 10^{-10}$ Torr at the opposite end).

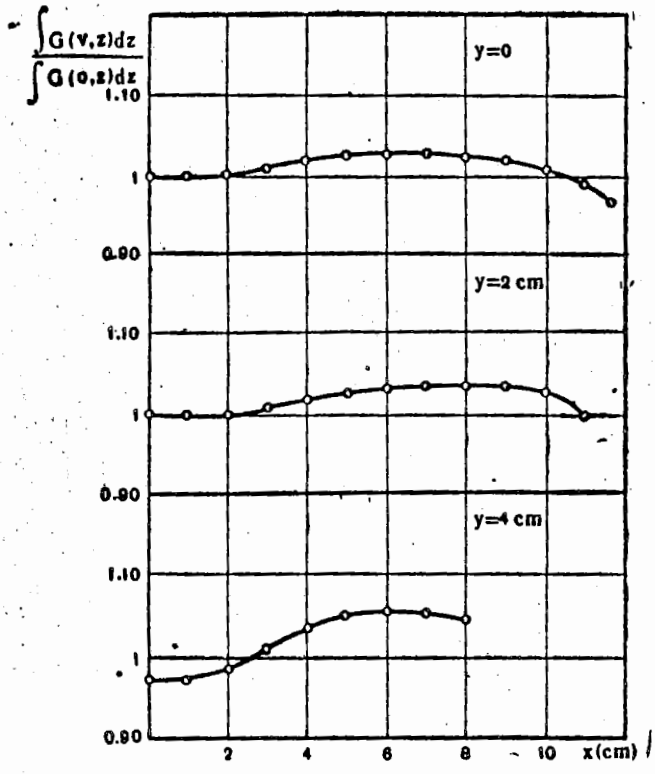

Fig. 16. Gradient integrated over the length measured on the quadrupole model. I — 40A, G (0, 0)—94 Gs/cm.

6. RF SYSTEM

The RF system must supply to the circulating beams a peak total voltage per turn equal to 180 kV (or 250 kV) by means of two (or three) resonant cavities, at a frequency of 8.9 MHz. The system as the diagram in Fig. 18 shows, is being designed for three cavities. The design must take care of two characteristic requirements of a storage ring; high reliability of operation and high beam loading. Accordingly the whole system is designed with large safety factors and the shunt dynamic impedance of the resonant cavities is quite low, of the order of 250 kΩ.

The output from the pilot oscillator goes to the three power amplifiers, via three phase shifters remotely controlled; each power amplifier is composed of four amplification stages, all of them in class B1 (with negligible grid current), in such a way that the amplitude modulation can be done at every power level. The amplifier bandwidth, defined as the region where the amplitude response is constant within $\pm 10^{-2}$, is 1 MHz.

The RF power that can be delivered to the load is equal to 50 kW per amplifier; the last stage is directly coupled to the resonant cavity. The resonant cavity is a two-folded cavity in air; corresponding to the two gaps the stainless steel donut will be interrupted with two alumina insulators, which must withstand 45 kV each and, at the same time, must keep the ultrahigh vacuum. A full scale model of the resonant cavity (Fig. 19) has been built and tested at low voltage (about 1/4 of the final voltage); a prototype of the power amplifier is almost completed (Figs. 20 and 21) and it will be used to test the resonant cavity in the operating conditions.

7. BUILDINGS

The layout of the linac and storage ring buildings is shown in Figs. 22 and 23. As the experiments are made on the ring itself, no experimental hall is needed; at the interaction regions a cilindrical volume, 2 m in radius and 2,5 m long, will be free for experimental apparatus. The ring is not on the linac axis, to allow an increase of its energy for future uses. Two experimental halls for the use of the linac beam will be provided on the other side of the linac tunnel; one at the end of the high current section and the other one at the end of the whole linac. The construction work, on the ground adjacent to the existing Laboratory site, began at the end of May, 1963; the present status can be seen in Fig. 24. The excavations for the linac tunnel and ring building foundations will be completed by the end of July, 1963; the linac tunnel is scheduled to be built in 12 months and the ring building in about 20 months.

REFERENCES

1. Amman F. et al. Proposta per la realizzazione di un anello di accumulazione per elettroni e positroni da 1.5 GeV. Laboratori Nazionali di Frascati, Report LNF 61/65, 7.12.1961.
2. Amman F. et. al. Elementi di progetto di un anello di accumulazione per elettroni e positroni da 750 MeV. Laboratori Nazionali di Frascati, Report LNF 63/34, 7.5.1963.
3. Gatto R. On the experimental possibilities with colliding beam of electrons and positrons.

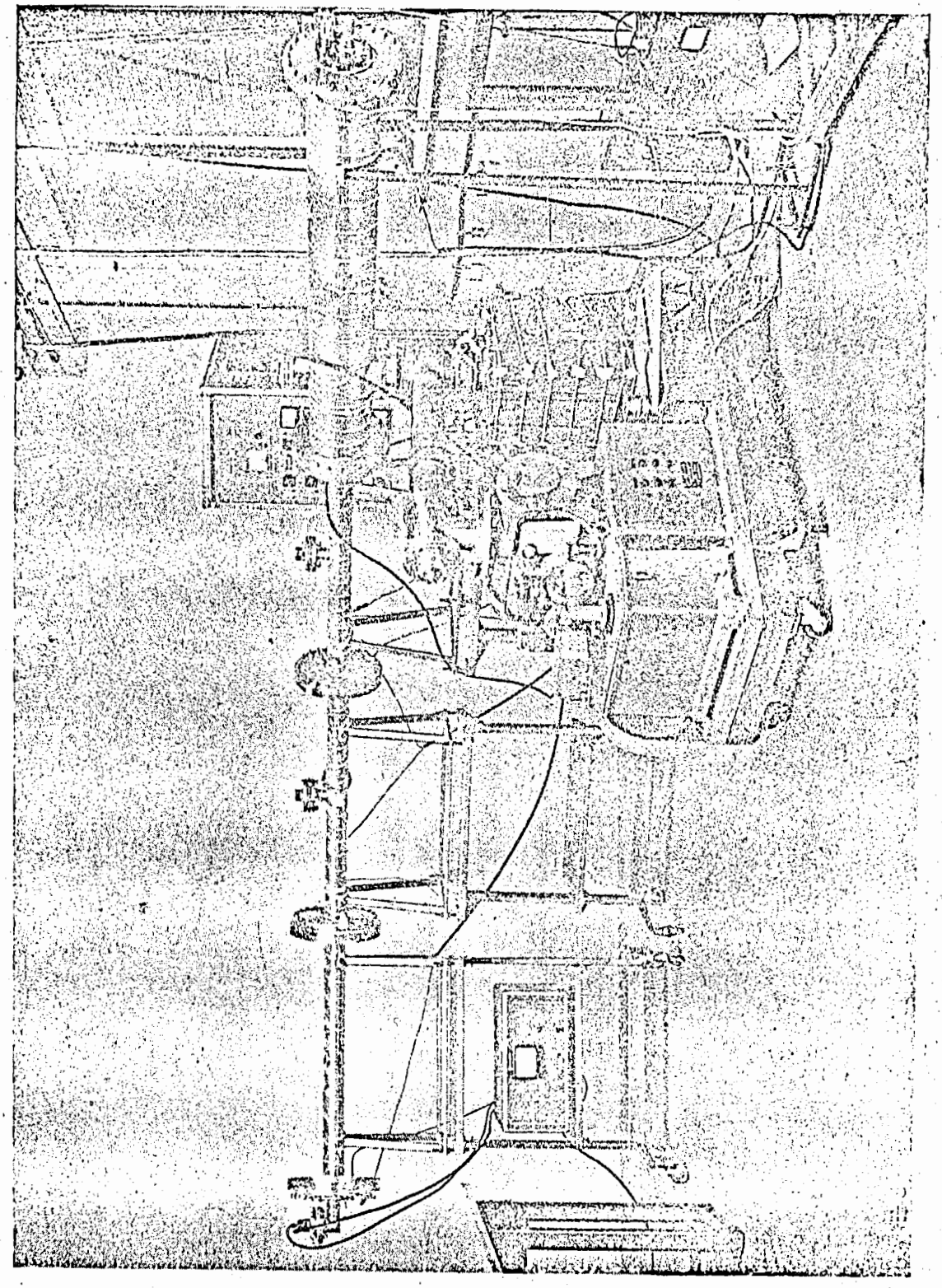

Fig. 17. Prototype of 1/24 of the donut.

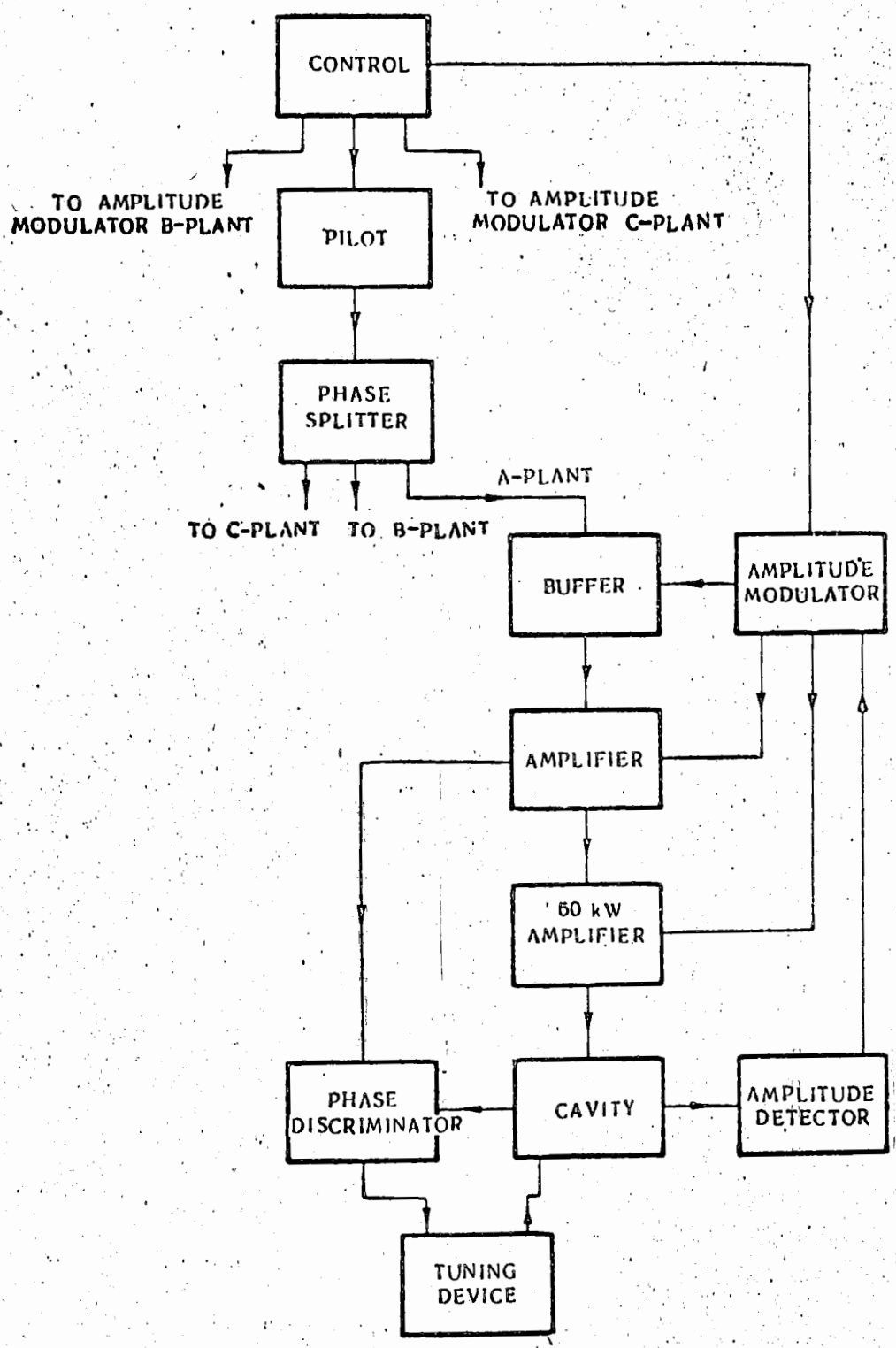

Fig. 18. RF system schematic diagram.

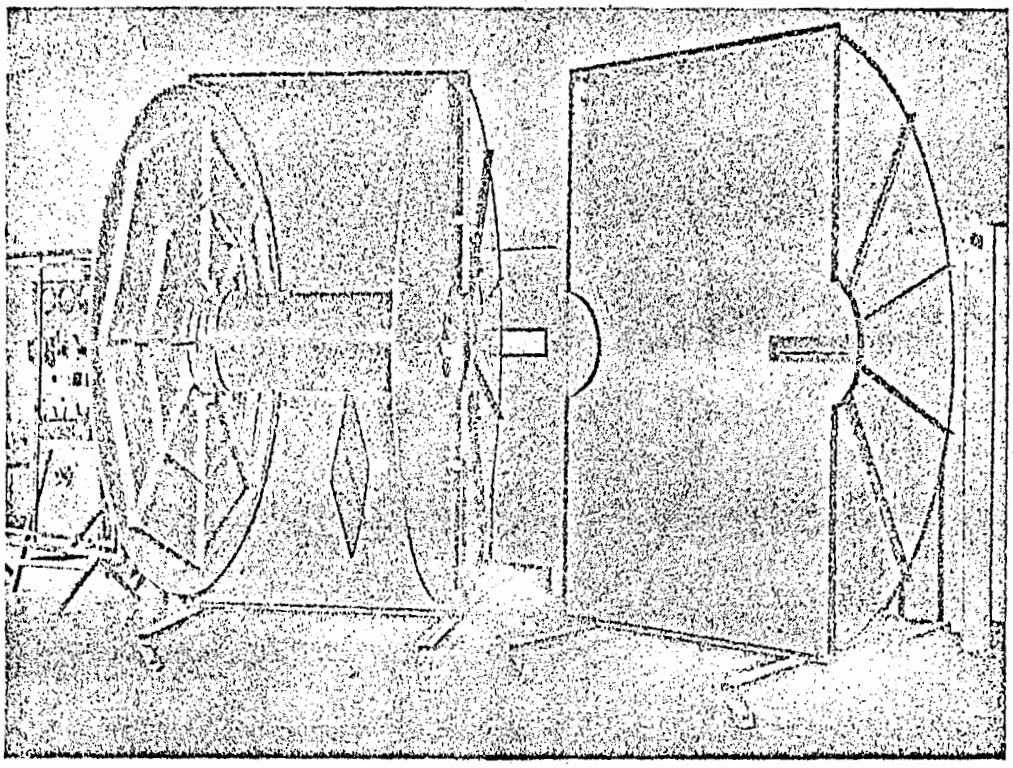

Fig. 19. Resonant cavity model.

In Proceedings of the Aix-en-Provence Conference, 1961, p. 487.
4. Cabibbo N., Gatto R. Phys. Rev., 124, 1577 (1961).
5. Amman F., Ritson D. Space charge effects in electron-electron and positron-electron colliding or crossing beam rings. In Proceedings of the International Conference on High Energy Accelerators (Brookhaven, 1961), p. 471.
6. Bassetti M. Calcoli numerici sugli effetti di carica spaziale in un anello di accumulazione per elettroni e positroni, Laboratori Nazionali di Frascati, Report LNF 62/35, 5.5.1962.
7. Pellegrini C. Nuovo cimento (Suppl.), 22, 603 (1961).
8. Pellegrini C. Non-linear effects on the damping constants of electron oscillations in a synchrotron. Laboratori Nazionali di Frascati, Report LNF 62/96, 21.II.1962.
9. Bernardini C. et al. Phys. Rev. Lett., 10, 407 (1963).
10. Bernardini C. et al. Lifetime and beam size in electron storage rings. See this edition, p. 332.
11. Aggson T. L., Burnod L. Labor. d'Orsay, Report LAL-27, October 1962.
12. Barber W. C. et al. An experiment on the limits of quantum electrodynamics. Stanford University, Report HEPL-170, June 1959.
13. Kuiper B., Plass G. On the fast extraction of particles from a 26 GeV proton synchrotron. CERN Report 59/30, 24.8.1959.
14. Courant E. D., Snyder H. S. Annals of Phys., 3, 1 (1958).
15. Cattoni A. Misure preliminari relative alle precisioni ottenibili nell'allineamento di Adone. Laboratori Nazionali di Frascati, to be published.

ДИСКУССИЯ DISCUSSION

С. А. Хейфец

На какую величину можно сместить частоты бетатронных колебаний в описанной установке?

F. Amman

In our ring it will be possible to change the betatron frequency by more than one unit; in practice, during operation, it will be needed a change of the order of 0.2.

С. А. Хейфец

Предусмотрена ли компенсация зависимости $\nu(E)$? Если да, то как вводится квадратичная нелинейность?

F. Amman

We do not think that such corrections are necessary.

А. А. Наумов

Какова мощность, излучаемая пучком электронов, в накопительном кольце?

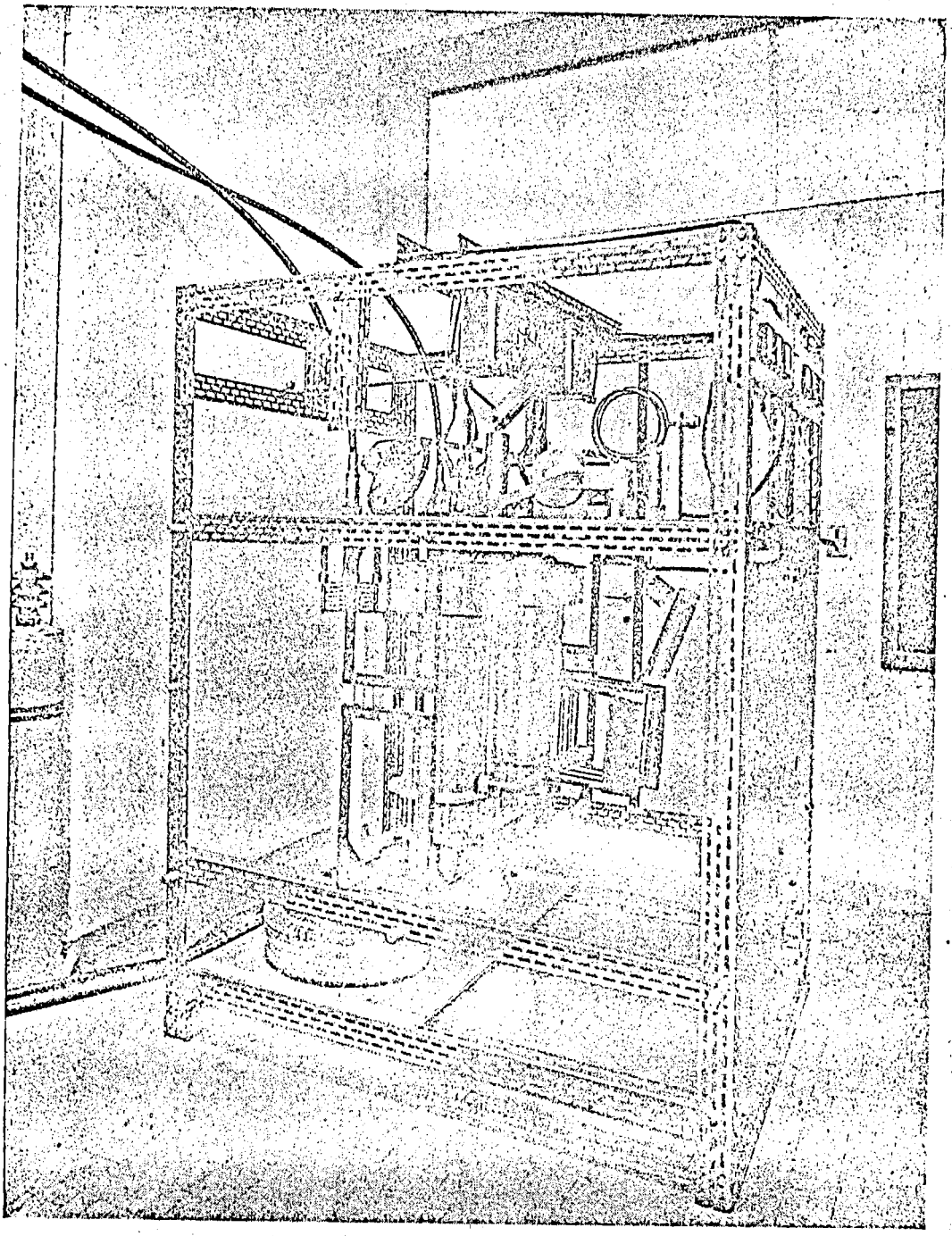

Fig. 20. RF power amplifier prototype.

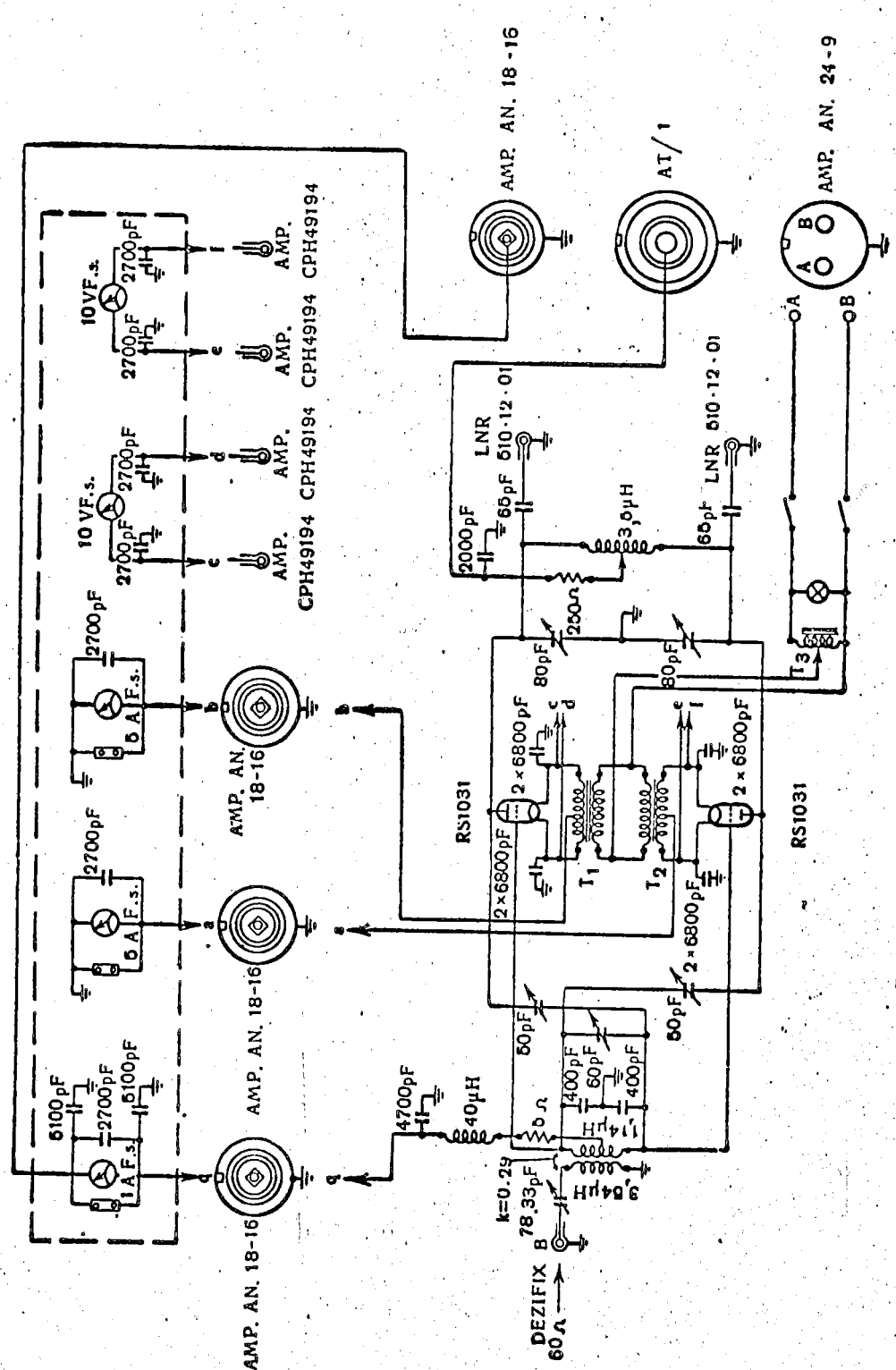

Fig. 21. Diagram of the RF power amplifier prototype.

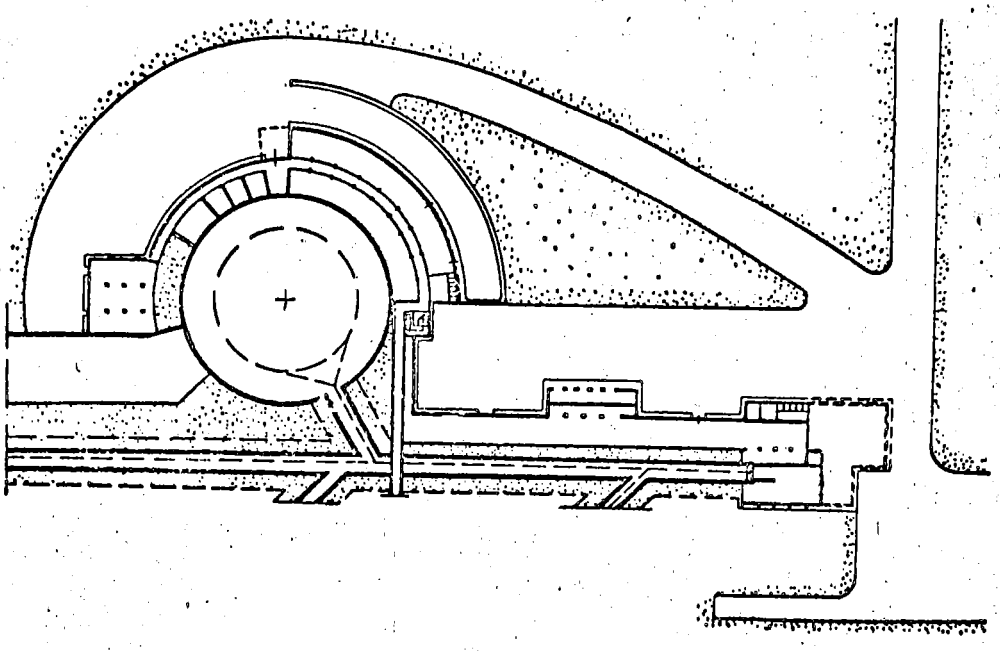

Fig. 22. Linac and storage ring building layout.

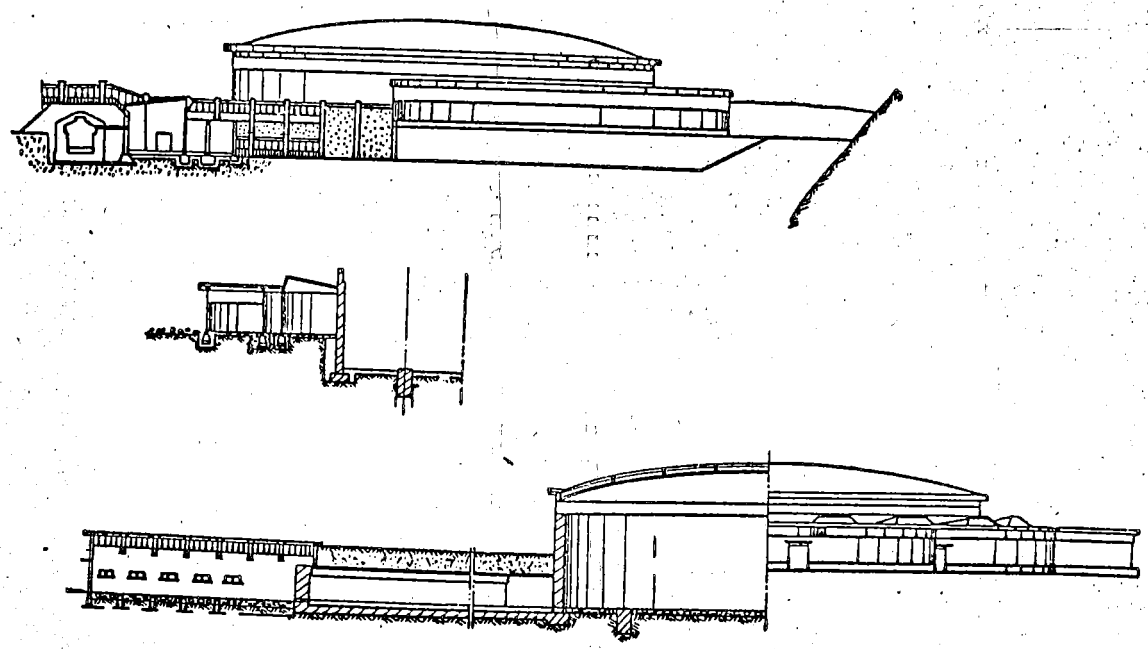

Fig. 23. Artist's view of the linac and storage ring buildings.

Fig. 24. Aerial view of the storage ring site.

F. Amman

The energy lost per turn is 90 keV, and the power which goes into light and soft γ-rays is about 20 kW.

Н. И. Мочешников

Согласно данным, представленным вами, величина электронного тока составит около 25 *ма*, а позитронного — 0,1 — 0,2 *ма*. Каким образом достигается такой высокий коэффициент преобразования электронов в позитроны?

F. Amman

The linac is composed of two parts: the first one can deliver on a tungsten target 420 mA of electrons at an energy of 65 MeV. The second one can accelerate a max. current of 100 mA. For this reason the ratio between the positron and electron currents available at the end of the linac is not connected to the conversion efficiency.